



HAL
open science

Modeling floods in a dense urban area using 2D shallow water equations

Emmanuel Jean Marie Mignot, André Paquier, S. Haider

► **To cite this version:**

Emmanuel Jean Marie Mignot, André Paquier, S. Haider. Modeling floods in a dense urban area using 2D shallow water equations. *Journal of Hydrology*, 2006, 327 (1-2), p. 186 - p. 199. 10.1016/j.jhydrol.2005.11.026 . hal-00452214

HAL Id: hal-00452214

<https://hal.science/hal-00452214>

Submitted on 1 Feb 2010

HAL is a multi-disciplinary open access archive for the deposit and dissemination of scientific research documents, whether they are published or not. The documents may come from teaching and research institutions in France or abroad, or from public or private research centers.

L'archive ouverte pluridisciplinaire **HAL**, est destinée au dépôt et à la diffusion de documents scientifiques de niveau recherche, publiés ou non, émanant des établissements d'enseignement et de recherche français ou étrangers, des laboratoires publics ou privés.

Author-produced version of the article published in Journal of Hydrology
2006, 327(1-2), 186-199.

The original publication is available at <http://www.sciencedirect.com/>
doi : 10.1016/j.jhydrol.2005.11.026

1 Modeling floods in a dense urban area using 2D shallow water equations

2 Mignot E¹., Paquier A²., Haider S³.

3 4 Abstract

5 A code solving the 2-D shallow water equations by an explicit second-order scheme is used to
6 simulate the severe October 1988 flood in the Richelieu urban locality of the French city of Nîmes. A
7 reference calculation using a detailed description of the street network and of the cross sections of the
8 streets, considering impervious residence blocks and neglecting the flow interaction with the sewer
9 network provides a mean peak water elevation 0.13 m lower than the measured flood marks with a
10 standard deviation between the measured and computed water depths of 0.53 m. Sensitivity analysis of
11 various topographical and numerical parameters shows that globally, the results keep the same level of
12 accuracy, which reflects both the stability of the calculation method and the smoothening of results.
13 However, the local flow modifications due to change of parameter values can drastically modify the
14 local water depths, especially when the local flow regime is modified. Furthermore, the flow
15 distribution to the downstream parts of the city can be altered depending on the set of parameters used.
16 Finally, a second event, the 2002 flood, was simulated with the calibrated model providing results
17 similar to 1988 flood calculation. Thus, the article shows that, after calibration, a 2-D model can be
18 used to help planning mitigation measures in a dense urban area.

19
20 **Keywords :** Flood; 2D shallow water equations; Calibration; Urban areas; Sensitivity analysis.

¹ PhD student, Cemagref, Hydrology-Hydraulics Research Unit, 3 bis quai Chauveau, CP220 , 69336 Lyon Cedex 09, France.

Email : mignot@lyon.cemagref.fr, *ph.* : +33 472208775, *fax* +33 478477875

² Researcher, Cemagref, Hydrology-Hydraulics Research Unit, 3 bis quai Chauveau, CP220 , 69336 Lyon Cedex 09, France.

Email : andre.paquier@cemagref.fr, *ph.* : +33 472208775, *fax* +33 478477875

³ Assistant Profesor, National Institute of Transportation, Risalpur, NWFP, Pakistan

1

2 **Introduction**

3 Surface flood modeling in urban environment is a challenging task for a number of reasons: the
4 presence of a large number of obstacles of varying shapes and length scales, the storages in the
5 buildings, the complex geometry of the city, etc. However, if the intensity of the event is strong
6 enough and the domain is a dense urban zone, it can be assumed that the majority of the flow passes
7 by the streets and the junctions. The flow in the streets is mostly one-dimensional except near the
8 junction but it was shown that at junctions (Weber et al., 2001) and bifurcations (Neary et al., 1999),
9 the flow is basically 3D. Thus (Huang et al., 2002) performed a 3D calculations of flow at a junction
10 and found that the results agreed with the measurements. However, (Khan et al., 2000) and (Shettar
11 and Murthy, 1996) showed that 2-D models can simulate the water surface and velocity field near the
12 crossing and predict the distribution at a subcritical bifurcation.

13 Looking at the available literature in surface urban flood simulations, this statement seems accepted by
14 many authors as it appears that most studies use 2-dimensional models. (Ishigaki et al., 2004) for an
15 experimental urban flood case study and for real cases use full shallow water equation models or
16 simplified models neglecting the inertial terms (Chen et al., 2004) to simulate urban floods. For these
17 real cases, the origin of the flood can be the overflow of a river (Calenda et al., 2003), the invasion of
18 land drainage flow from the upstream hills (Aronica and Lanza, 2005; Haider et al., 2003), the rain
19 storm event on the modeled area or sewer drainage failure (Hsu et al., 2000; Mark et al., 2004; Schmitt
20 et al., 2004). The building blocks can be either considered impervious or numerical methods for
21 introduction of flow in the building blocks are proposed (Inoue et al., 2000). In most of the urban
22 flooding numerical simulation references, only few validation data was available and so the quality of
23 the simulations could not be precisely assessed. Furthermore, calibration processes and the influence
24 of the chosen parameters were not proposed in the previously cited references.

1 In order to examine the conditions of use of a 2-D model, the authors decided to investigate the case of
 2 the dense city of Nîmes that experienced two recent dramatic flood events in a topographical context
 3 of steep slopes and high velocities. The explicit finite volume numerical code “Rubar 20” (Paquier A.,
 4 1995; Paquier A., 1998) was used to solve the full 2D shallow water equations. The October 1988
 5 flood was used as a base simulation in order to discuss the sensitivity of such a calculation to
 6 particular modeling features: the level of detail in the description of the streets, the description of
 7 specific urban structures, the boundary conditions, the values of some numerical parameters. Then
 8 modeling of a second event (the September 2002 flood) was performed in order to validate the
 9 calibration of the model. Finally, a conclusion about the calibration process of such a model and its
 10 technical application for planning emergency measures is undertaken.

11

12 The governing equations and the numerical scheme

13 The system of 2D shallow water equations consists of 3 equations: one equation for continuity and two
 14 equations for the conservation of momentum in the two orthogonal directions.

$$15 \quad \frac{\partial h}{\partial t} + \frac{\partial(hu)}{\partial x} + \frac{\partial(hv)}{\partial y} = 0 \quad (1)$$

$$16 \quad \frac{\partial(hu)}{\partial t} + \frac{\partial(hu^2)}{\partial x} + \frac{\partial(huv)}{\partial y} + gh \frac{\partial h}{\partial x} = -gh \frac{\partial z_b}{\partial x} - gn^2 \frac{u \sqrt{u^2 + v^2}}{h^{1/3}} + \nu_{ef} \frac{\partial}{\partial x} \left(h \frac{\partial u}{\partial x} \right) + \nu_{ef} \frac{\partial}{\partial y} \left(h \frac{\partial u}{\partial y} \right) \quad (2)$$

$$17 \quad \frac{\partial(hv)}{\partial t} + \frac{\partial(huv)}{\partial x} + \frac{\partial(hv^2)}{\partial y} + gh \frac{\partial h}{\partial y} = -gh \frac{\partial z_b}{\partial y} - gn^2 \frac{v \sqrt{u^2 + v^2}}{h^{1/3}} + \nu_{ef} \frac{\partial}{\partial x} \left(h \frac{\partial v}{\partial x} \right) + \nu_{ef} \frac{\partial}{\partial y} \left(h \frac{\partial v}{\partial y} \right) \quad (3)$$

18 In which h is water depth, u and v are velocities along horizontal x and y -axis, z_b is bottom level, n is
 19 Manning’s roughness coefficient, g is gravity acceleration and ν_{ef} is effective cinematic viscosity.

20 Usually, it is assumed that the viscosity is constant throughout the flow field. However, the model
 21 (simpler than the k - ϵ model) defined by the following relation was also tested:

$$22 \quad \nu_{ef} = k h u^* \quad (4)$$

1 In which k is a non-dimensional coefficient and the bottom friction velocity u^* is approximated by (5)
2 instead of the usual relation from the friction coefficient in order to enhance the variations of the water
3 surface elevation.

$$4 \quad u^* = \sqrt{gh \sqrt{\left(\frac{\partial(z_b+h)}{\partial x}\right)^2 + \left(\frac{\partial(z_b+h)}{\partial y}\right)^2}} \quad (5)$$

5 In the “Rubar 20” code (Paquier A., 1995; Paquier A., 1998), the conservative form of the equations
6 (1) to (3) above are solved on a grid constituted of quadrilaterals and triangles using an explicit
7 second-order numerical scheme that is adapted from MUSCL approach (VanLeer B., 1979). The
8 selected scheme is able to calculate highly unsteady flows and can treat the transitions between
9 subcritical and supercritical flows as ordinary points. Drying and wetting of cells are treated
10 specifically in the following way: a cell is considered as dry as long as the water volume entering an
11 originally dry cell during one time step provides an average water depth in the cell below a minimal
12 value (0.01 μm in present study). During drying process, a similar option is used and leads to a mass
13 conservation error that is usually less than 0.01 % of the total mass. This numerical scheme is
14 generally stable under the Courant Friedrichs Levy condition that limits the Courant number to values
15 below unity. However, in the case of steep slopes, the time step should be further restricted; thus,
16 modeling requires high calculation power.

17 The validation of the numerical scheme on very unsteady flows (against analytical solutions and
18 experimental data sets) was extensively performed through the IAHR group on dam-break wave and
19 during the CADAM and IMPACT European research projects that included comparisons with other
20 numerical codes. Some of these experiments included dam beak wave calculation in simple
21 rectangular channels, in more irregular topography domains with introduction of blocks to simulate
22 obstacles or buildings (Mignot and Paquier, 2003a; Mignot and Paquier, 2003b) or on a real urban
23 flood situation (Mignot and Paquier, 2004). All these tests proved the relevance of “Rubar 20” code to
24 solve 2D shallow water equations in rapid flow and complex topographic situations. To complete the
25 code validation in the domain of urban floods, some experimental tests of four rectangular channel

1 junction flows were performed in the INSA Fluid Mechanics Laboratory in Lyon (France). Precise
2 measurements of the observed flow patterns of supercritical junction flows were performed and
3 compared to the water depths computed with “Rubar 20” (Mignot et al., 2005b). It appeared that the
4 code was able to predict with fair agreement the structure of the flow and the locations of the specific
5 flow structures such as the hydraulic jumps, the recirculation zones and the eddying (Mignot et al.,
6 2005a).

7

8 **The 1988 flood and the presentation of the studied area**

9 Nîmes is a French city located in a plain just downstream from 7 hills surrounding its northern area.
10 Since 1350, many records of severe floods have been recorded in the city and the flood of October, 3rd
11 1988 in Nîmes was among the most dramatic observed events. It was caused by a rainstorm that
12 generated up to 420 mm of rain in about eight hours on the northern hills (Desbordes et al., 1989) and
13 led to the overflow of the watercourses to the north of the city and the subsequent inundation of
14 various localities with water depths up to 3 meters, causing extensive damages to property and human
15 life (Bonneaud, 2002). (Desbordes et al., 1989) evaluated the return period of this event to 150 to 250
16 years.

17 The studied area known as “Richelieu”, located in the Northeastern part of the city of Nîmes was one
18 of the most dramatically affected zones. The dimensions of the area are about 1400 m along the north-
19 south axis that is also the main principal flow direction, and a variable East-West width with a
20 maximum and minimum of about 1050 m and 220 m respectively. A railway embankment runs all the
21 way along the northern side, the western flank is formed by hills and the eastern flank is constituted
22 by an impervious railway station (Figure 1). One particularity of the city of Nîmes is that no river
23 crosses the city, indeed when it rains on the region, the flow drained by the temporary watercourses
24 enters the urban area and flows in the underground watercourses until reaching the Vistre river
25 downstream from the city. However, when the discharges in the watercourses becomes larger than
26 their conveyances, overflows occur upstream from the city and the water enters its Northern parts

1 following the natural slope (north to south), flowing within the streets. “Richelieu” is one of these
2 localities, where the flow can enter through several street underpasses located in the railway
3 embankment. The drop in ground level in the studied area is respectively 20 and 15 m from the
4 western and eastern underpasses (Figure 1) to the southern boundary, which represents an average
5 slope higher than 1 %. The upstream part of the city (Figure 1) is composed of large building blocks
6 areas such as the military barracks and the hospital with wide streets and few crossroads. The central
7 part is a rather regular network with narrow streets (5 to 8 meters wide) and right angle crossings
8 between them. This area is interesting due to the relative abundance of the flood marks that
9 demonstrates an average peak water depth of about one and a half meter. However, photos show that,
10 in some specific points, waves occurred and water surface rose along the buildings, which means some
11 uncertainties in the peak water level, confirmed by differences between couples of close water marks
12 Finally, the urban structure of the Southern part is intermediate between the Northern and Central part,
13 with average width streets and still a high main North-South slope.

14

15 **Available data for the 1988 flood and their preliminary processing**

16 The Public works department of the Gard County and the Technical Services of Nîmes city supplied
17 the necessary primary data for the simulations. It included:

- 18 (a) About 200 cross-sectional profiles for the 60 streets located in the studied area. A typical street
19 profile (Figure 2) contained 11 points including the top and foot of both side walls (points 1
20 and 2), both pedestrian ways (points 3), both gutters (points 4 and 5) and the mid point of the
21 road section (point 6).
- 22 (b) A map of the area showing the limits of the flooded area, the land use (built-up places...) and
23 some complementary ground elevations. The 99 flood mark elevation points measured
24 immediately after the 1988 flood were also noted on the map showing the measurement
25 locations. 85% of these flood marks are located in crossroads at the corner between two
26 building walls and the remaining 15% are located within the streets on the façade of a building.

1 (c) Rainfall data measured at various locations around the area.

2 BCEOM French consulting firm performed an hydrological modeling (BCEOM et al., 2004) on the
3 upstream basins (10 km² and 3.5 km²) starting from rainfall measurements in order to compute
4 hydrographs at the upstream border of the Richelieu domain. The model is based on a conceptual
5 linear tank approach similar to GR4 model (Perrin et al., 2003); it considers separately the
6 hydrological processes on the urban areas and the runoff on grass land of the upstream basins. Then,
7 for various hydrological events, the model was calibrated to fit with the observations of flood marks at
8 the upstream end of the Richelieu area (railway line) and more upstream.

9 In this step, the sewage network was taken into account, the discharge capacity of the sewage network
10 (4m³/s and 7m³/s for the pipes at the Western and Eastern domain entrance respectively) was
11 subtracted form the calculated surface inflow hydrographs. Nevertheless, it appears that the maximum
12 capacity of the sewage network is less than 10 % of total peak discharge in 1988, which is of the order
13 of the hydrological results uncertainties. Furthermore, when the upstream hydrograph reached the
14 studied area, the sewage network was already almost full due to the rain falling on the city. The result
15 of this hydrological modeling consists in two discharge hydrographs that can be used for inputs at the
16 northwest and northeast upstream boundary of the model. The hydrographs span a period of 13 hours
17 with a time step of 15 minutes (Figure 3).

18 The cross-sectional street profiles (Figure 2) constituted the basic structure of the calculation mesh. In
19 order to obtain a complete description of the city, a linear interpolation between the intersecting streets
20 permitted to obtain the input and output cross sections of each street junction. Then the generation of
21 the 121 points of each crossroad (11 points from both joining streets) was achieved by interpolating
22 between the input and output sections. Additional points and information were introduced for the mesh
23 of the "complex" topographical crossings. Building blocks were considered as watertight and details
24 about them were not introduced. Furthermore, the sewage network was not taken into account in the
25 hydraulic study, assuming that the exchanges between the surface and the network could be neglected

1 compared to the flow rates and water depths in the streets. From this construction, the DEM contains
2 about 25,000 points for the streets, each one described by its three coordinates x, y, z .

4 Reference calculation

5 The basic calculation mesh is generated keeping all the points from the DEM and adding extra points
6 along the streets. The specification of an average space step of 25 meters along the streets generally
7 leads the mesh generator to interpolate less than five additional sections along the streets. This choice
8 of a rather long space step came from the hypothesis that, except in (or close to) the crossings, the
9 flow is predominantly 1D. Furthermore, this reduces the calculation time but restricts the possibilities
10 to include small scale urban structures and to simulate the complexity of the flow in the streets in the
11 vicinity of the junctions. The mesh consists of 100 quadrangles in each crossroad and between 30 and
12 60 quadrangles in each street reach (10 across each street multiplied by 3 to 6 along the street).

13 The parameters were set to their default values that *a priori* was considered as the best initial way to
14 obtain suitable results. Friction was estimated to have uniform Manning's coefficient on the whole
15 area accounting for the actual flow friction on the road pavement and the building walls and for the
16 interaction of the flow with various small scale obstacles (trees, cars, bus stops...). The corresponding
17 information available in the literature for 2D simulations in street networks can vary much : Manning
18 coefficients used were $n=0.01$ (Aronica and Lanza, 2005), $n=0.015$ (Nania, 1999), $n=0.025$
19 (Gourbesville and Savioli, 2002), $n=0.043$ (Inoue et al., 2000) and $n=0.08$ (Calenda et al., 2003).

20 Values of friction coefficient $n= 0.025 \text{ s.m}^{-1/3}$ and diffusion coefficient of $0.1 \text{ m}^2/\text{s}$ were chosen for our
21 case. The calculation was performed with a fixed time step of 0.01 s. The hydrographs presented in
22 Figure 3 constitute the upstream boundary conditions at both streets passing below the railway
23 embankment at the northern end of the domain. In order to limit the calculation time, only the initial
24 10 hours of the hydrographs were considered for the simulation. This duration is sufficient to capture
25 the flood dynamics and to obtain the peak water levels at any point in the modeled area. Also, the rain
26 on the domain is neglected. A critical flow boundary condition (Froude number equal to one) was

1 fixed at the downstream ends of the model, i.e. the six downstream streets (*S3* to *S7* on *Figure 1*)
2 oriented from North to South, the three streets (*S8* to *S10*) oriented West to East and the three (*S1* and
3 *S2* on *Figure 1*) oriented East to West. An additional outlet with free flow condition was added in a
4 street at the Eastern end of the domain (*S11*) in order to take into account overflows to a railway line
5 located more than one meter below the model boundary.

6 The domain is initially dry and at the beginning of the event, both hydrographs invade the area on each
7 side of the northern part of the domain. Part of the Eastern discharge flow turns towards the Eastern
8 limit of the area and then leaves the calculation domain through the exit *S11* located in *Pitot street*. On
9 the other hand, a large part of both upstream flows joins at the *Faita/Sully* crossroad and spreads in the
10 Central zone narrow streets and into the Southern part of the domain before leaving the area at the
11 Southern limits. Most of the streets are flooded by the flow from the upstream to the downstream
12 reach of the street, however, some streets such as the Western part of *Pitot street* are filled through
13 their downstream reach due to backwater effects. The time of maximum water depth in most places
14 corresponds to the peak of the Eastern hydrograph (*Figure 3*), which intensity is much larger than the
15 Western hydrograph. At the flood peak ($t \sim 4.1$ hours), high velocities (3 to 4 m/s) and supercritical
16 regime flow occur along the main North-South slope directions especially in the wide streets and low
17 velocities (0.5-0.7 m/s) with subcritical regimes appear in the streets aligned West to East (*Figure 4*).
18 In the crossroads, the flow is generally complex and both regimes can be observed. On the other hand,
19 the maximum depths appear in two locations : in the *Faita* street at the sudden street narrowing and in
20 the *Faita/Sully* crossroad (*Figure 5*). Those two locations also correspond to low velocity zones.

21

22 **Comparison of calculation results with observations**

23 First it appears that the extent of the flooded area (*Figure 5*) is in agreement with the limits supplied by
24 the officials of the Gard County as it is mostly determined by topographical limits (hills and building
25 walls).

26 In Nîmes, the flood marks were recorded on the building walls. However, in our numerical model, no
27 water depth calculation is performed on the cell edges and the 99 flood marks had to be compared with

1 the peak water depths calculated at the center of the nearest cell, which is on the “pedestrian walk”
2 cell. These cells are named “*comparison cells*” in the following paragraphs. The results of the peak
3 water depths comparison are given in Table 1. About 40% of the peak water depths are overestimated
4 and 60% underestimated by the calculation, the largest difference being about 1.6 meters and the
5 average absolute difference is 41 cm.

6 The model appears to be calibrated on the Northern part of the domain (Table 1) where the average
7 difference between the computed peak water depths and the flood marks is close to 0, even though the
8 standard deviation is large (56 cm). The peak water depths at two main locations appear not to be
9 fairly estimated : the Eastern entry (zone A) where the water depth of the flow below the railway
10 embankment is underestimated and upstream from one of Faita crossroads (zone B) where the sudden
11 reduction of the street width may not be represented accurately in the interpolated mesh. In the Central
12 part of the domain, the computed peak water depths in the narrow streets are strongly underestimated
13 (zone C) by an average of 43 cm (Table 1). This underestimate may be due to the street characteristics:
14 narrow streets with many parked cars reducing the flowing section and increasing locally the friction.
15 Finally, the peak water depths in the Southern area is slightly overestimated ($dh = 13$ cm in Table 1);
16 however this overestimate is mainly due to the overestimate of the water depth in one street (zone D in
17 Figure 6) where topographical uncertainties or other flow features may have occurred.

18 The histogram (Figure 7) showing the peak water depth differences between calculation
19 results and on-site measurement is centered around 0 proving that no specific bias is
20 encountered.

21

22 Sensitivity test cases

23 The influence of various parameters was tested on the 1988 flood event by altering just one parameter
24 in each calculation compared to the reference case simulation, by checking the induced modifications
25 in the numerical results and explaining the origins of the changes. From a general point of view,
26 Figure 8 shows that the shapes of the computed limnigrams remain all quite similar but, when looking

1 at the error table (Table 1), it appears that the prediction of the peak water depth at the 99 comparison
2 locations (flood mark locations) can be strongly affected by the choice of the parameters set.

3 4 *Case 1 : Inflow and storage of water*

5 Case 1A. In order to check the influence of the hydrological calculation uncertainties, the input
6 discharge hydrographs were increased by an amount of 20% at each time step compared to the
7 reference calculation. The consequence of such increase in upstream input condition is an average
8 increase of water depth (of 12.5 cm), with a larger increase in the upstream zone (17cm) than the
9 Central and downstream zones (10 cm each) because of higher damping of peak discharge
10 downstream.

11 Case 1B. In the reference case, the only water input considered is the drainage from the upstream
12 watersheds. In case 1B, the rain falling on the streets and building blocks (supposed to reach
13 instantaneously the closest street cells) was added. Although the intensity of the rain is very high
14 (maximum of 61 mm/h), the rain water volume remains low (212,000 m³) compared to the input
15 hydrographs volume (3,600,000 m³) and its influence is very limited : the peak water depths are
16 increased everywhere by about 4 cm, i.e. 4%. The strongest influences are observed in the downstream
17 part of the domain (due to cumulative effects) and in the streets filled by backwater effects at the
18 downstream reach (*Pitot street*).

19 Case 1C. In the reference case, it was assumed that all the buildings were impervious and that water
20 could not be stored in caves, courtyards, dead end streets... However, witnesses and photographs
21 reveal that the water actually invaded most of these areas reducing the volume of water flowing in the
22 streets. Among the storage areas in the domain, the military barracks area represents the largest
23 storage volume available and a calculation with its gate completely open was launched. The computed
24 volume stored at the flood peak is about 80,000 m³ which is very small compared to the input volume
25 of 3,600,000 m³. Consequently, apart from local flow modifications near the gate, only a very small
26 reduction of computed peak water depths (about 1 cm) occurs in the areas downstream from the
27 military barracks.

1

2 *Case 2 : Friction and viscosity numerical coefficients*

3 Case 2A. Energy is dissipated numerically through the bottom friction and diffusion that should
4 mainly reflect both the effect of turbulence and the heterogeneity along the vertical direction. In order
5 to check the influence of the diffusion coefficient ν_{ef} in equations (2) and (3), we simulated the event
6 applying, on the one hand a 0 diffusion coefficient and on the other hand a coefficient depending on
7 the water depth as presented in equation (4) with $k=10^{-2}$. For this latter value 60% of the cells have an
8 equivalent diffusion coefficient ν_{ef} larger than 0.1 m²/s at the flood peak. The results from these two
9 calculations show that the diffusion parameter has a very small influence on the computed flow, the
10 average absolute peak water depth modification being about 3 cm on the studied area.

11 Case 2B. Identifying the exact friction coefficient is almost impossible as this coefficient stands for the
12 sum of various sources of resistances such as bottom friction, friction on the walls or due to their
13 irregularities, small scale obstacles to the flows. The $n=0.025$ Manning coefficient first chosen was
14 changed to $n= 0.033$.

15 1) Overall, this larger friction tends to increase all the computed peak water depths of about 10 cm.

16 2) Nevertheless, it also modifies strongly the flow structure in the vicinity of *Faita/Sully* crossroad
17 with the consequence of altering the flow distribution at this junction. Indeed this larger friction
18 coefficient lowers the flow discharge – thus decreasing the peak water depths - in the downstream
19 *Faita* street and modifies the flow distribution in the downstream boundary streets. Consequently, the
20 computed flood in the whole Southern area is affected.

21 3) Finally, the change in friction coefficient slightly alters the predicted flow structure in most
22 crossroads and, in some cells, the flow regime can be changed between supercritical and subcritical
23 conditions, hence strongly modifying the local computed water depths. For instance Figure 9 presents
24 the flow regimes computed at one crossroad at the flood peak for the Reference case and Case 2B and
25 shows that the flow in the comparison cell is supercritical for the Reference case and subcritical for
26 Case 2B. Consequently, for Case 2B the water depth at this time is the maximum water depth

1 computed during the event but for the Reference case, the water depth is lower than before $t=3.8h$ and
2 after $t=4.8h$ (Figure 10).

3 In the end, it appears that considering the $n=0.033$ friction coefficient, the underestimation of peak
4 water depths is decreased in the Central zone but then overestimations appear in the Northern zone and
5 increase in the Southern zone. Globally, the computed average peak water depth is less underestimated
6 than the reference case (Table 1) but then the model is not any more calibrated in the Northern zone
7 ($\overline{dh} = 17\text{ cm}$) and becomes more overestimated in the Southern zone.

8 Case 2C. The improvement of the results in the Central zone presented in the previous paragraph leads
9 us to consider different friction coefficients for the various zones of the urban area. The friction
10 coefficient in the narrow streets of the Central zone (all except *Faita* and *Semard* streets) is increased
11 to $n=0.05$ (and $n=0.025$ remains in the rest of the domain). Indeed, as the streets are narrower in this
12 zone, the relative importance of the building walls friction increases; moreover, the presence of many
13 parked cars creates a stronger resistance to the flow. As was expected, in the Central zone, the
14 velocities are decreased and the peak water depths increased, improving their comparison with the
15 flood marks (Table 1). This test proves that the friction parameter should be calibrated for each
16 homogeneous urban zone according to the potential friction due to the fixed and mobile (non
17 represented) obstacles and the street dimensions.

18

19 *Case 3 : Downstream boundary conditions*

20 Case 3A. The change of the numerical treatment of the downstream boundary condition from a critical
21 flow condition (Froude number = 1) to a free condition (corresponding to a local zero discharge
22 gradient hypothesis in case the flow regime is subcritical, and no flow influence if the local flow is
23 supercritical) strongly alters the flow in the close vicinity of the domain downstream limit: the
24 computed flow depths are strongly increased and the flow distribution to the downstream streets is
25 highly modified.

1 Case 3B. Besides, it was considered, in the reference case, that the flow could leave the studied
2 domain without being influenced by the further downstream parts of the city. However, a large part of
3 the city was flooded during the event and some backwater effects from the downstream neighbor
4 streets may have occurred especially around the flood peak. Then, a calculation was performed
5 assuming very strong downstream South-Eastern and South-Western urban zone influences : the flow
6 was prevented from leaving the domain through streets *S1*, *S2* and *S10* (Figure 1). This drastic change
7 of downstream boundary condition has a strong effect on the flow in the whole Southern part of the
8 city : the peak water depths are increased in the closed streets (*S1*, *S2* and *S10*)due to a local storage
9 of water volume and also near the other downstream streets as more outflow discharge occurs. As a
10 result, the computed peak water depth becomes strongly overestimated both in the southern part of the
11 Central zone (due to backwater effects) and in the Southern zones (Table 1 and Figure 11).

12 To sum up, whereas the choice of numerical method to calculate the downstream boundary condition
13 has only a space influence on the computed flow limited to the last downstream streets, the choice of
14 the streets allowing outflow from the domain to the downstream zones can alter strongly the flow in
15 the whole downstream area up to the fourth street towards the upstream direction.

16

17 *Case 4 : Topographical modifications without altering the mesh*

18 Case 4A. In order to simplify the data processing or if the available topographical data are not precise
19 enough, one can assume the street sections as being flat, thus neglecting the real profile of the streets.
20 In order to check the influence of this simplification, the bottom elevation of each street node was set
21 equal to the corresponding street mid-point bottom elevation. Two tendencies are then observed for
22 the 99 comparison cells :

23 1) Globally, the water depths are increased by about 10 cm in the whole studied area. Indeed,
24 we remark that the water volume in the street is similar to the reference case and generally, on the
25 comparison cells both the water depth and water level are increased, see Figure 12.

1 2) The topographical modification of the crossroads topography can affect strongly the local
2 flow and the flow regime can change with the consequence of strong local water depth modification
3 (see Figure 10).

4 Overall, it appears that the comparison between computed peak water depths and the flood marks is
5 improved in the underestimated zones, namely the Central zone and worsened in the Northern and
6 Southern zones.

7 Case 4B. Another important question in urban flood modeling is whether it is worth representing
8 precisely the topography of the complex crossroads (or squares). A calculation was made by
9 simplifying drastically the topography of the *Faita/Sully* crossroad (to which more than 75% of the
10 flood flow converges) considering that the junction between both streets is a simple quadrilateral area
11 obtained by interpolating both streets sections as for the other simple crossroads. As could be expected
12 the flow structures and thus the computed water depths within the crossroad are much affected.
13 Moreover, it appears that :

14 1) The water depths in the upstream streets are increased as the reduction of the flowing section
15 creates backwater effects towards the upstream area.

16 2) The flow distribution in the downstream streets of the crossroad is modified due to a change of the
17 flow pattern at the junction : the discharge in *Faita* street is increased by 31% whereas the discharge in
18 *Sully* street is decreased by 10%. As a consequence, the peak water depths are globally increased in
19 *Faita* street and slightly decreased in *Sully* street.

20 Case 4C. Finally, when a large amount of small scale debris (cars, fences...) is available in a zone,
21 some important obstacles can form downstream. In order to check the influence of such an obstacle, an
22 impervious wall was set at the downstream end of a main slope street of the central area (dot line in
23 Figure 1). The following consequences are observed. First, a storage of water just upstream from the
24 obstacle causes a large increase of water depth in the street and backwater effects increasing the water
25 depths in the upstream streets. Also, the original discharge of this street is re-directed towards the
26 neighbor streets, also increasing the water depths. Finally, the water volume downstream from the
27 obstacle is reduced and the computed water depths are lowered. Overall, it appears that the strong

1 influence of the obstacle is spatially restricted, the maximum discharges modification in the
2 downstream boundary streets is only $2\text{m}^3/\text{s}$ (i.e. 8 %). Nevertheless, for flood events as strong as the
3 1988 flood, several such obstacles can happen in various places and in the end can have a strong
4 influence on the peak water depths on the whole area.

5 6 *Case 5 : Mesh density in a longitudinal direction (same profile description)*

7 Two tests were performed to check the influence of the mesh density in the longitudinal street
8 direction without altering the mesh density of the streets profile and at the crossroads: The first test
9 (Case 5A) mesh consists on only one calculation cell in each street portion between two crossroads,
10 with the interest of reducing the calculation time. For the second test (Case 5B), the longitudinal mesh
11 comprises an average of 4 to 5 cells in each street. The comparison between the computed peak water
12 depths and the flood marks located in the streets has no meaning as the calculation points are too
13 different. Concerning the flood marks in the crossroads (85% of the marks), the absolute average peak
14 water depths are almost not affected by the mesh refinement (absolute average change of 2.5cm) and
15 only slightly affected (by about 8.5 cm) when using the coarser longitudinal mesh. The causes for
16 these modifications are: first, some local flow structure modifications in the junction along with some
17 changes of flow regimes as for cases 2B and 4A (Figure 10); then a modification of flow distribution
18 at *Faita/Sully* crossroad, increasing the South-Western flow rates and decreasing it in the South-
19 Eastern area and finally a strong change in backwater effect in Pitot street flooded by a downstream
20 filling.

21 22 *Case 6 : Simplification of street profile mesh*

23 Altering the number of points used in the street profiles leads to the generation of different meshes and
24 to a variation of the profile topography (Figure 13) seven (Case 6A), five (Case 6B), and four points
25 (Case 6C) were considered. In going from an 11-points cross-section to a 4-point cross-section, the

1 number of wetted calculation cells at the crossroads decreases from 64 to 1, and the amount of data
2 required to mesh the urban area and the calculation time is also reduced.

3 For all the simplifications of the street section (cases 6A, 6B and 6C), a tendency similar as for case
4 4A (to a smaller extent) appears : the computed water depths are slightly increased on the whole
5 domain due to an increase of the average bottom elevation of the street section. Moreover, for the 4-
6 points cross-sections case (and also 5-points in a smaller extent), another phenomenon is observed :
7 the small amount of cells in the crossroads simplifies drastically the flow structure. Then the local high
8 or low velocity areas within the junction disappear and only the average flow regime remains. For
9 instance, if the flow in the crossroad is mainly subcritical with a small supercritical area in a corner
10 (where the flood mark is located), then the 4-points cross-section case will compute an average
11 subcritical flow at the junction and thus overestimate the peak water depth (compared to the flood
12 marks and the reference case results). This phenomenon observed at 5 comparison cells locations is
13 presented in Figure 14. The opposite phenomenon can also occur if the flow is globally supercritical in
14 the junction with just a small subcritical area. Besides, the local modifications in the computed flow
15 also influence drastically the flow at larger scales and in the 4-points section cases, it alters the flow
16 distribution to the downstream boundary streets as shown in Figure 15.

17 To sum up, it appears that the 7-points cross-section computation results show a very small peak water
18 depths modification on the whole studied area whereas these results with 4-points and 5-points cross-
19 section computation are very affected by the street profile mesh simplification (Table 1).

20

21 **Validation of the model calibration on the 2002 flood event**

22 Apart from the October 1988 flood, the September 2002 event was among the largest flood observed
23 in the past decades in Nîmes. The event process was roughly similar to the 1988 case with a rainfall
24 intensity much lower and thus an available volume also reduced. BCEOM company applied a similar
25 hydrological method in order to obtain both input hydrographs. In this case, the 2002 sewer network
26 capacities is of the order of the flow rates coming from the upstream watersheds ($6\text{m}^3/\text{s}$ and $7\text{m}^3/\text{s}$

1 compared to $13\text{m}^3/\text{s}$ and $30\text{ m}^3/\text{s}$) and both pipes capacities were subtracted from the original input
2 hydrographs. 28 flood marks were measured on building walls after this event, with an average peak
3 water recorded of about 30 cm and a maximum of 85 cm in *Faita* street.

4 The parameters set used in the 1988 reference case is used to simulate the 2002 event using the same
5 mesh with the appropriate input hydrographs (Figure 16). It appears from the computed results that the
6 flood dynamics is quite similar as the one described for the 1988 case, even though all water depths
7 are much lower. The comparison between the computed peak water depths and the flood marks is
8 given in Figure 17.

9 It appears that the errors in peak water depth computation are quite homogeneously
10 distributed in the studied area, and no spatial tendency can be observed. Indeed, contrary to
11 the former case, the water depths in the narrow streets network of the Central zones are not
12 underestimated. Furthermore, the average error between computed and recorded peak water
13 depths is $\overline{dh} = -3\text{cm}$ proving that the calibration of the model is accurate for the simulation of
14 the September 2002 flood event. However, the large standard deviation ($\sigma_{dh} = 22\text{cm}$) shows
15 that some local phenomenon must have modified the flow locally. Indeed, with the lower
16 water depths in the streets, the small scale obstacles, topographical irregularities and storage
17 areas have a larger influence on the flow for this less extreme flood.

18

19 **Conclusions and recommendations**

20 2D shallow water equations in their complete form were solved to simulate the flood propagation
21 through an urban area represented as a network of streets. Street profiles including its main structural
22 elements were used to mesh the streets and crossroads. Other features such as obstacles (cars, bus
23 stops...), flood water storage spaces (cellars, parkings...) were not considered but could be introduced
24 in order to obtain more realistic local results (Haider, 2001; Haider et al., 2003). A first case of severe
25 urban flood (1988 case) for which the exchanges between the streets and the potential storage areas or

1 the sewage network are globally negligible was used for calibration and in order to check the influence
2 of various numerical and topographical parameters on the computed flow. The numerical results
3 obtained show a standard deviation of about 50 cm. This is rather high but reflects the uncertainty in
4 the flood marks, the insufficiency of the topographical data provided initially, and, may be, the local
5 influence of somewhat hazardous events such as blockages by cars or building walls irregularities for
6 instance. Concerning the sensitivity analysis, it appeared that some parameters had very limit effects
7 and others had larger effects on the flow structure and especially the computed peak water depths.
8 Furthermore, some parameter modifications have global, zonal or local influences. Table 2 sums-up
9 the impacts of the various parameters tested in this article but the conclusions will not necessarily be
10 the same in other flood situations.

11 Consequently, the following recommendations could be useful for modelers wishing to simulate a
12 severe urban flood in a dense urban area :

13 1) Special attention should be paid during the hydrological calculations to establish the input
14 hydrographs. Especially, the peak discharge of the hydrographs should be precisely calculated if the
15 first objective is to establish the map of the peak water depths on the area.

16 2) If the rain volume falling on the studied area or the storage volume available in the domain are
17 small compared to the input hydrographs volumes, their effects will be very small and it is not worth
18 representing them.

19 3) Different friction coefficients should be applied for the various homogeneous urban feature zone,
20 depending on the width of the streets and the fixed and mobile obstacles that may increase the
21 resistance to the flow.

22 4) Collecting information about the flooded areas just downstream from the studied zone is
23 important in order to set accurate limit boundary conditions at the downstream streets.

24 5) The refinement of the mesh to be used for the calculation depends strongly on the objectives of
25 the study. If the main objective is to have an overview of the flood dynamics, then a rough description
26 of the street profile seems accurate enough. In the case of the 1988 flood, the 5-points cross-section
27 points with 3 wetted cells longitudinally between two crossroads seem a good compromise.

1 Nevertheless in this case, the modeler should keep in mind that a slight global water depth
2 overestimation (about 10 cm) occurs on the whole studied domain due to the increased average street
3 profile bottom elevation. The main advantages of considering a coarse mesh is both to simplify the
4 topographical data collection on the area and to reduce the calculation time, often prohibitive when
5 trying to simulate precisely an urban flood. However, if information about local velocities and/or
6 water depths exists in order to use this data for model calibration, then a more precise description of
7 the streets is required. In this case, it seems that the representation of the gutters is not required and the
8 use of 7-points crossing-sections (4 wetted cells in the section), thus with 49 nodes and 32 wetted cells
9 in each crossroad should be accurate enough except in the complex crossroads where specific attention
10 have to be paid to mesh the local topography more precisely.

11 Finally, the calibrated model was validated on a second less extreme event: the September 2002 flood.
12 The results show a standard deviation of about 20 cm, which is better than for the 1988 flood case but
13 is high compared to the average peak water depth in the area (about 30 cm). One reason for this may
14 be the higher sensitivity of the model to the small scale irregularities of the topography.

15 These results on one particular flood case should be confirmed on other field or experimental cases
16 showing a similar complicated pattern of streets and crossings. However, it was shown that the use of
17 a code solving 2-D shallow water equations to assess flood risk in a city seems a convenient solution.

18 In the case of Nîmes, the results of such calculations are being used for the reorganization of buildings
19 in the Richelieu area for urban projects ("Hoche – Sernam" operations). The new urban planning are
20 taken into account to modify the mesh of the studied area and calculations with the calibrated model of
21 a flood event equivalent to the 1988 case permit to check the peak water depths modifications.

22

23 **Acknowledgements**

24 This study has been funded by French Ministry of Environment through the two projects of the
25 program "Flood Risks" entitled "Hydrological risk in the urban environment" and "Estimation of

1 surface flows for an extreme flood in urbanized environment". Many thanks should also be addressed
2 to all the partners of these two projects.

3

4

5 **Notations**

6 dh difference between computed peak water depth and flood mark measurement

7 \overline{dh} average of dh

8 F = Local Froude number

9 g gravity acceleration

10 h water depth

11 k non-dimensional coefficient in viscosity calculation

12 n Manning's roughness coefficient

13 u velocity along horizontal x -axis,

14 u^* bottom friction velocity

15 v velocity along horizontal y -axis,

16 z_b bottom level

17 ν_{ef} effective kinematic viscosity.

18 σ = Standard deviation

19

1

2 **References**

3

- 4 Aronica, G.T. and Lanza, L.G., 2005. Drainage efficiency in urban areas: a case study. *Hydrological*
5 *Processes*, 19.
- 6 BCEOM, CS and Météo France, 2004. Outil de prévision hydrométéorologique - Projet Espada - Ville
7 de Nîmes (Technical report in French).
- 8 Bonneaud, S., 2002. Nîmes, du 3 octobre 1988 au Plan de Protection Contre les Inondations (CD rom),
9 Publisher : Agropolis International, Proceeding of conference : "Inondations en France",
10 Montpellier, France (in French).
- 11 Calenda, G., Calvani, L. and Mancini, C.P., 2003. Simulation of the great flood of December 1870 in
12 Rome. *Water and Maritime Engineering*, 156(4).
- 13 Chen, H.H., HSU, M.H. and Chen, T.S., 2004. The integrated inundation model for urban drainage
14 basins, Novatech 2004, Lyon, France.
- 15 Desbordes, M., Durepaire, P., Gilly, J.C., Masson, J.M. and Maurin, Y., 1989. 3 Octobre 1988:
16 Inondations sur Nîmes et sa Région: Manifestations, Causes et Conséquences (in French).
17 Publisher : C. Lacour, Nîmes France.
- 18 Gourbesville, P. and Savioli, J., 2002. Urban runoff and flooding : interests and difficulties of the 2D
19 approach, 5th international Hydroinformatics (2002), Cardiff, UK.
- 20 Haider, S., 2001. Contribution à la modélisation d'une inondation en zone urbanisée. Approche
21 bidimensionnelle par les équations de Saint Venant (in French). (Contribution to the
22 modelling of a flood in an urbanised zone - 2-D approach by de Saint Venant equations) . Ph
23 D Thesis, Institut National des Sciences Appliquées, Lyon.
- 24 Haider, S., Paquier, A., Morel, R. and Champagne, J.-Y., 2003. Urban flood modelling using
25 computational fluid dynamics. *Water and Maritime Engineering*, 156(2).
- 26 Hsu, M.H., Chen, S.H. and Chang, T.J., 2000. Inundation simulation for urban drainage basin with
27 storm sewer system. *Journal of hydrology*, 234.
- 28 Huang, J.C., Weber, L.J. and Lai, Y.G., 2002. Three-dimensional numerical study of flows in open-
29 channel junctions. *Journal of Hydraulic Engineering-Asce*, 128(3).
- 30 Inoue, K., Kawaike, K. and Hayashi, H., 2000. Numerical simulation models of inundation flow in
31 urban area. *Journal of Hydrosience and Hydraulic Engineering*, 18(1).
- 32 Ishigaki, T., Nakagawa, H. and Baba, Y., 2004. Hydraulic model test and calculation of flood in urban
33 area with underground space, *Environmental Hydraulics and Sustainable Water Management-*
34 *Lee & Lam (eds) : Volume 2, Sustainable Water Management in the Asia-Pacific Region,*
35 *A.A. Balkema Publishers.*
- 36 Khan, A.A., Cadavid, R. and Wang, S.S.Y., 2000. Simulation of channel confluence and bifurcation
37 using the CCHE2D model. *Water and Maritime Engineering*, 142.
- 38 Mark, O., Weesakul, S., Apirumanekul, C., Aroonnet, S.B. and Djordjevic, S., 2004. Potential and
39 limitations of 1D modelling of urban flooding. *Journal of hydrology*, 299.
- 40 Mignot, E. and Paquier, A., 2003a. Impact - Flood propagation case study - The model city flooding
41 experiment, 3rd IMPACT Workshop (EU-funded research project on Investigation of Extreme
42 Flood Processes and Uncertainty), Louvain La Neuve, Belgium. 5-7 November 2003.
43 Publisher : HR Wallingford.
- 44 Mignot, E. and Paquier, A., 2003b. Impact - Flood propagation. Isolated building test case, 3rd
45 IMPACT Workshop (EU-funded research project on Investigation of Extreme Flood Processes
46 and Uncertainty), Louvain La Neuve, Belgium, 5-7 November 2003. Publisher : HR
47 Wallingford.
- 48 Mignot, E. and Paquier, A., 2004. Impact-Flood propagation case study. The flooding of Sumacárcel
49 after Tous Dam Break. Cemagref's modelling, 4th IMPACT Workshop (EU-funded research
50 project on Investigation of Extreme Flood Processes and Uncertainty), Zaragoza, Spain, 3-5
51 November 2004. Publisher : HR Wallingford.

- 1 Mignot, E., Paquier, A., Perkins, R.J. and Rivière, N., 2005a. Flow structures at the junction of four
2 supercritical channel flows, 10th International Conference on Urban Drainage, Copenhagen,
3 Denmark, 21-26 August 2005.
- 4 Mignot, E., Paquier, A. and Rivière, N., 2005b. 2D numerical simulation of four branches
5 experimental supercritical junction flows, XXXI IAHR Congress, 11th - 16th September
6 2005, Seoul, Korea.
- 7 Nania, L.S., 1999. Metodologia numérico-experimental para el analisis del riesgo asociado a la
8 escorrentia pluvial en una red de calles. PhD Thesis, Universitat politècnica de Catalunya,
9 Barcelona (in Spanish).
- 10 Neary, V.S., Sotiropoulos, F. and Odgaard, A.J., 1999. Three-dimensional numerical model of lateral-
11 intake inflows. *Journal of Hydraulic Engineering*, 125(2): 126-140.
- 12 Paquier A., 1995. Modélisation et simulation de la propagation de l'onde de rupture de barrage (in
13 French) (Modelling and simulating the propagation of dam-break wave). PhD Thesis,
14 Université Jean Monnet de Saint Etienne.
- 15 Paquier A., 1998. 1-D and 2-D models for simulating dam-break waves and natural floods. In :
16 Concerted action on dam-break modelling, processings of the CADAM meeting (ed. by
17 M.Morris, J.-C. Galland, and P. Balabanis). European Commission, Science Research
18 Development, Hydrological and hydrogeological risks, Luxembourg.
- 19 Perrin, C., Michel, C. and Andreassian, V., 2003. Improvement of a parsimonious model for
20 streamflow simulation. *Journal of hydrology*, 279(1-4).
- 21 Schmitt, T.G., Thomas, M. and Ettrich, N., 2004. Analysis and modeling of flooding in urban drainage
22 systems. *Journal of hydrology*, 299.
- 23 Shettar, A.S. and Murthy, K.K., 1996. A numerical study of division of flow in open channels. *Journal*
24 *of Hydraulic Research*, 34(5).
- 25 VanLeer B., 1979. Towards the ultimate conservative difference scheme. V.A second order sequel to
26 Godunov's method. *Journal of computational physics*, 32.
- 27 Weber, L.J., Schumate, E.D. and Mawer, N., 2001. Experiments on flow at a 90° open-channel
28 junction. *Journal of Hydraulic Engineering*, 127(5).
- 29
30

- 1 Figure legends
- 2
- 3 Figure 1 : “Richelieu” area of the city of Nîmes with S_1 to S_{11} the outlets from the area
- 4 Figure 2 : 11-points street section profile
- 5 Figure 3 : East and West hydrographs at the studied area border for the 1988 flood.
- 6 Figure 4 : Supercritical and subcritical flow regimes at the peak of the flood
- 7 Figure 5: Water depths at the flood peak and limit of flooded area (in dot lines)
- 8 Figure 6 : Map of comparison between computed peak water depths and measured flood
- 9 marks with $dh = H_{max,computed} - H_{max,measured}$
- 10 Figure 7 : Histogram of peak water depth prediction error.
- 11 Figure 8 : Limnigrams at point P1(Figure 1) for various parameter set cases.
- 12 Figure 9 : Flow regime patterns at the flood peak ($t=4.1$ hours) in one crossroad for Reference
- 13 case and Case 2B
- 14 Figure 10 : Limnigrams computed at the comparison cell of Figure 9 for Reference case and
- 15 Case 2B.
- 16 Figure 11 : Comparison between the reference case and Case 3B computed water depths in
- 17 the Central and Southern zones of the domain with $dh = h_{3B} - h_{reference}$.
- 18 Figure 12 : Increase in water depth using a flat profile description
- 19 Figure 13 : 7- 5- and 4-points simplified profiles
- 20 Figure 14 : Comparison between flood mark and computed peak water depth for reference
- 21 and 4-points cross-section calculation at supercritical small scale zones of the crossroads
- 22 Figure 15 : Comparison of flow rate distribution in the downstream end streets for reference
- 23 and 4-points cases.
- 24 Figure 16 : Flood hydrograph for September 2002 flood event after subtracting the sewer
- 25 capacities.

1 Figure 17 : Comparison between peak water depths and measured flood marks

2

3

1

2 **Table legends**

3 Table 1 : Comparison between computed and measured peak water depth for the reference
4 case and some important parameters modification. \overline{dh} is the average difference between

5 computed and measured peak water depths: $\overline{dh} = \frac{\sum dh}{n} = \frac{\sum (H_{computed} - H_{measured})}{n}$ with $H_{measured}$

6 the flood mark measurement, $H_{computed}$ the computed peak water depth in the nearest cell and n
7 is the number of flood marks (99 in this case). σ_{dh} is the standard deviation of dh :

8
$$\sigma_{dh} = \sqrt{\frac{\sum (dh - \overline{dh})^2}{n}}$$

9 Table 2 : Impact of the main parameters in the sensitivity analysis with :

10 (1) = Global change of peak water depths (with \uparrow = increase and \downarrow = decrease of peak water depth)

11 (2) = Change in flow distribution at *Faita/Sully* crossroad and to the downstream limit areas

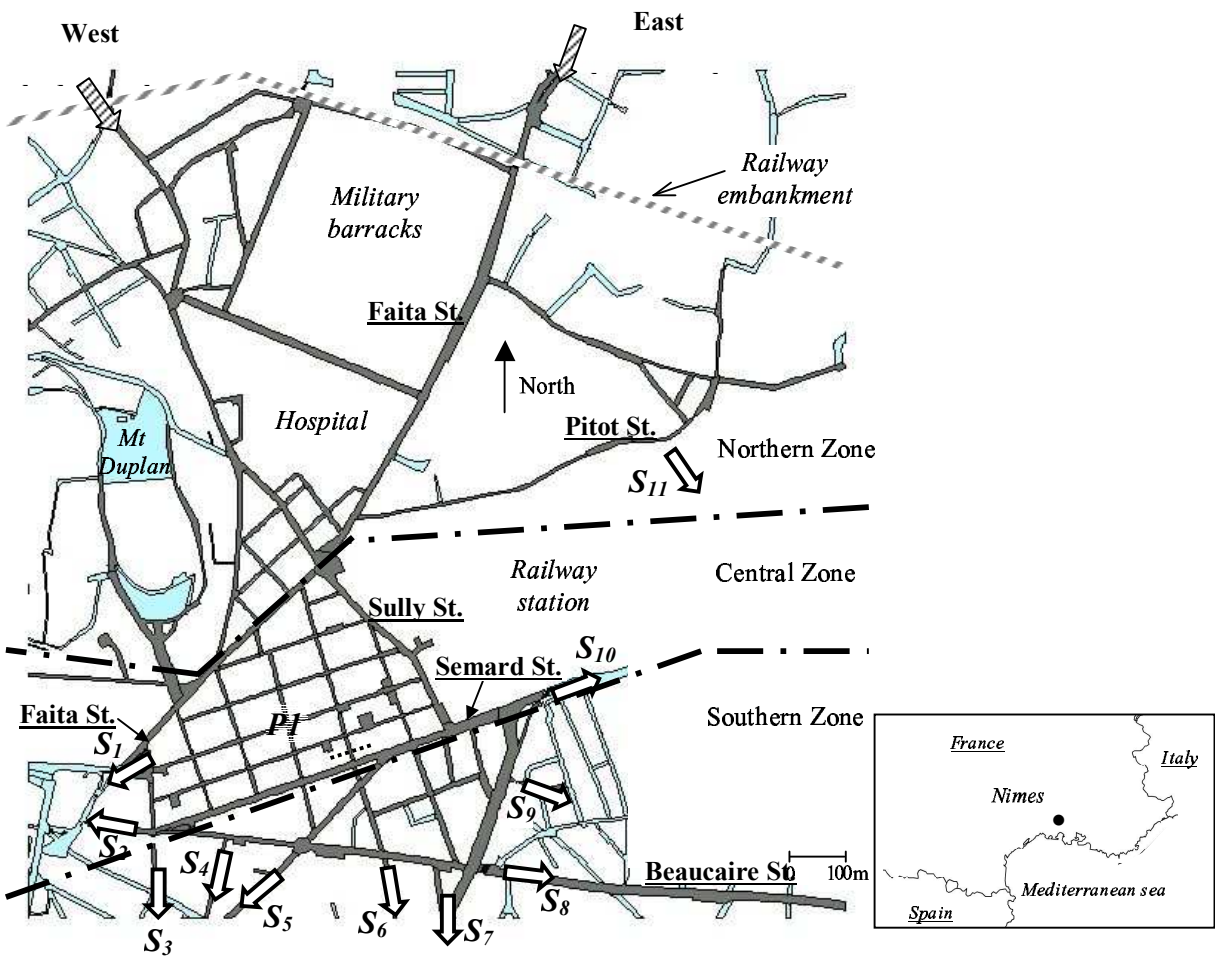
12 (3) = Local flow regime change

13

14

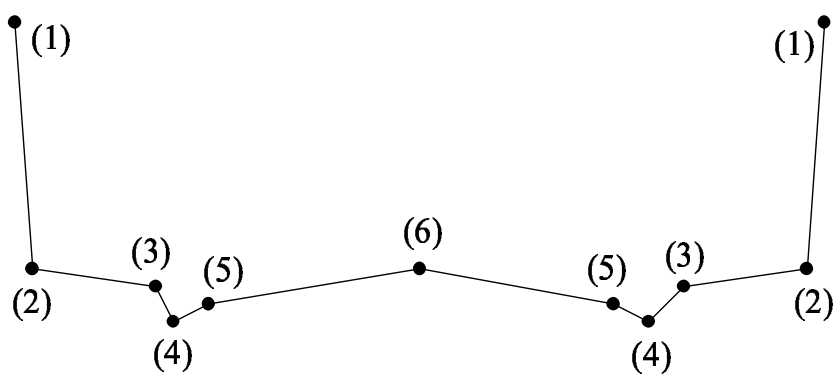
1 **Figures**

2
3
4
5
6
7
8
9
10
11
12
13
14
15



16 *Figure 1 : "Richelieu" area of the city of Nîmes with S₁ to S₁₁ the outlets from the area*

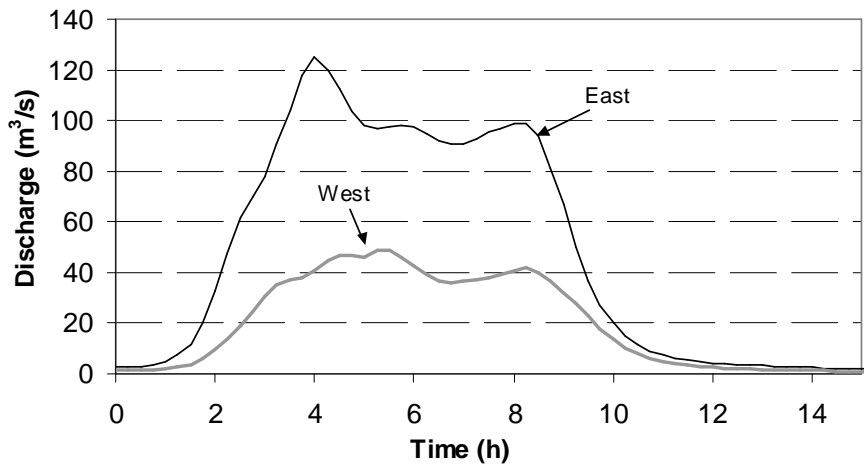
17



18

19 *Figure 2 : 11-points street section profile*

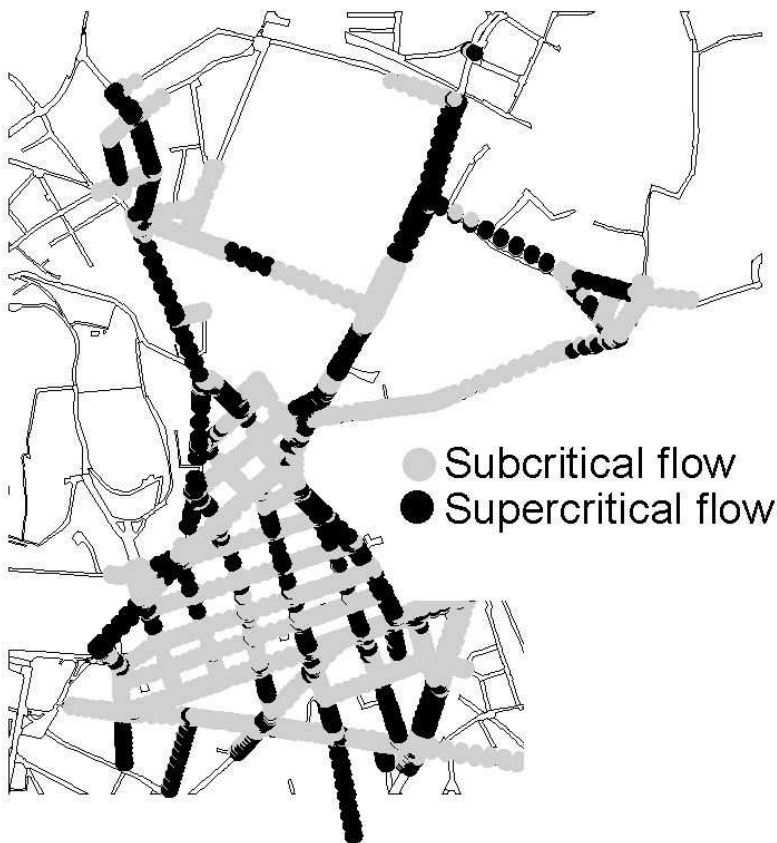
1



2

3 *Figure 3 : East and West hydrographs at the studied area border for the 1988 flood.*

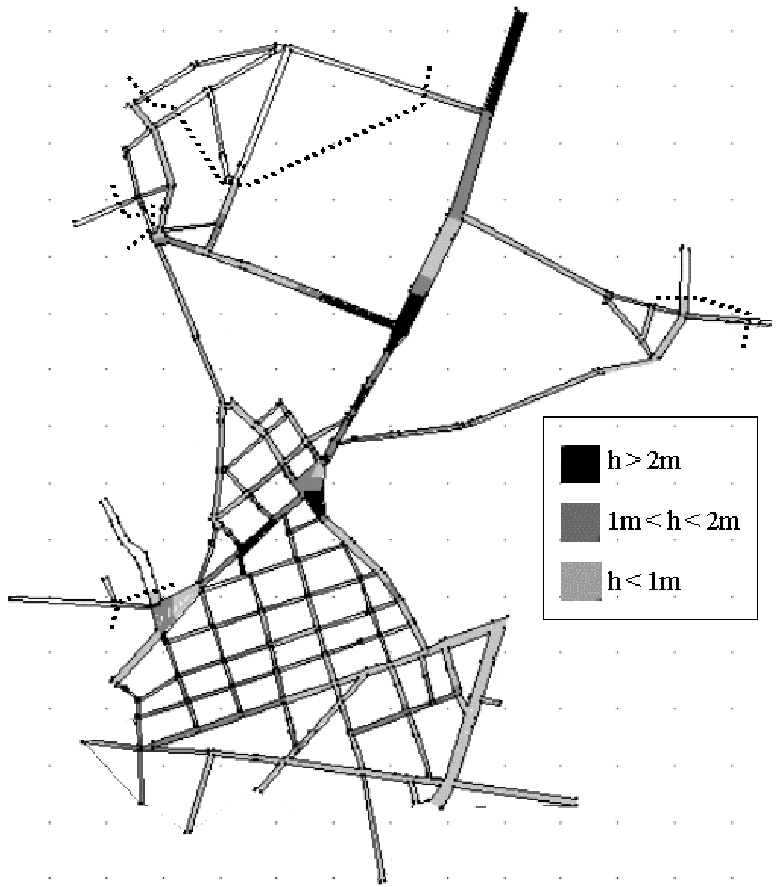
4



5

6 *Figure 4 : Supercritical and subcritical flow regimes at the peak of the flood*

1



2

3 *Figure 5: Water depths at the flood peak and limit of flooded area (in dot lines)*

4

5

6

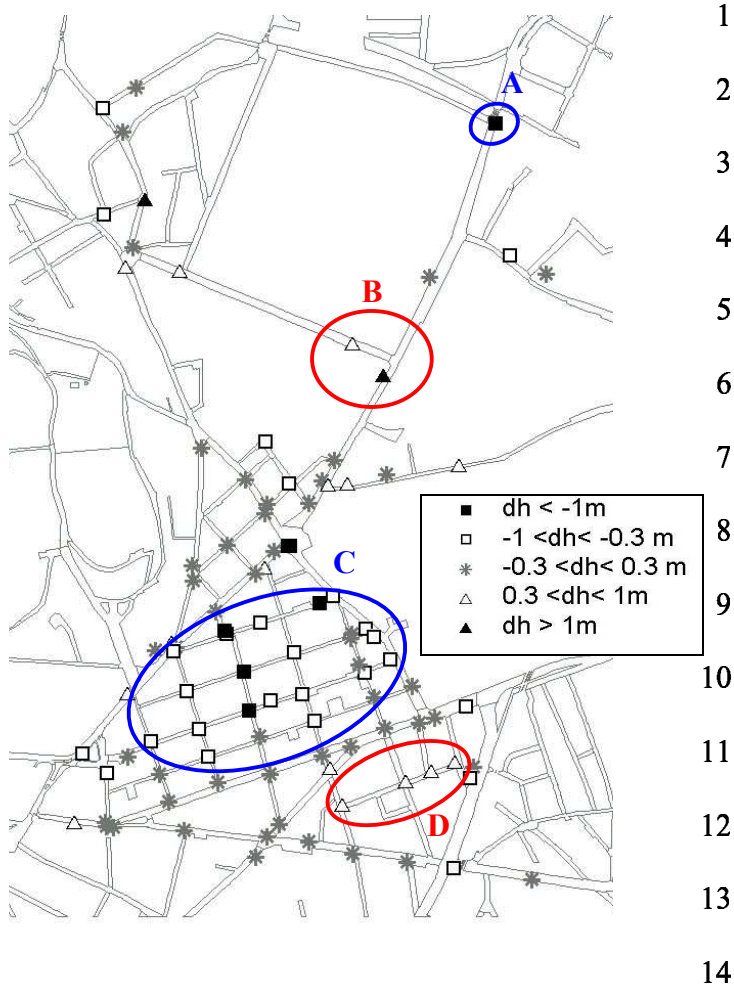
7

8

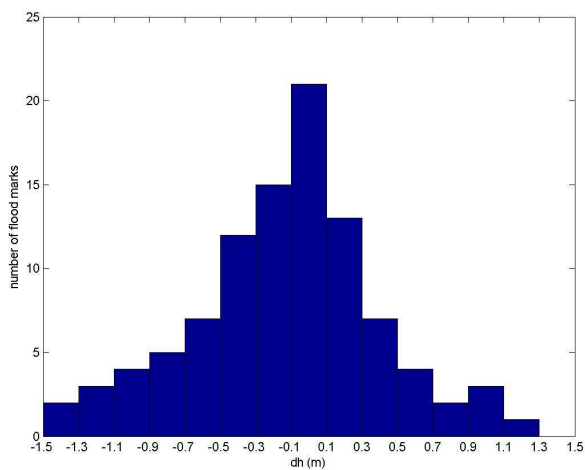
9

10

11



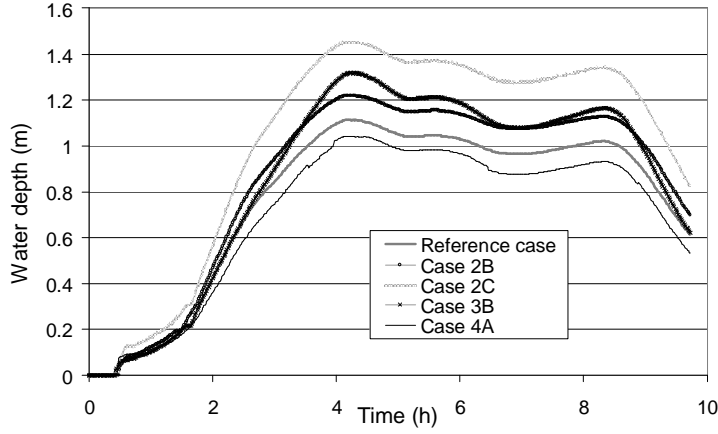
15 *Figure 6: Map of comparison between computed peak water depths and measured flood marks with*
 16 $dh = H_{max,computed} - H_{max,measured}$
 17



18

1 *Figure 7 : Histogram of peak water depth prediction error.*

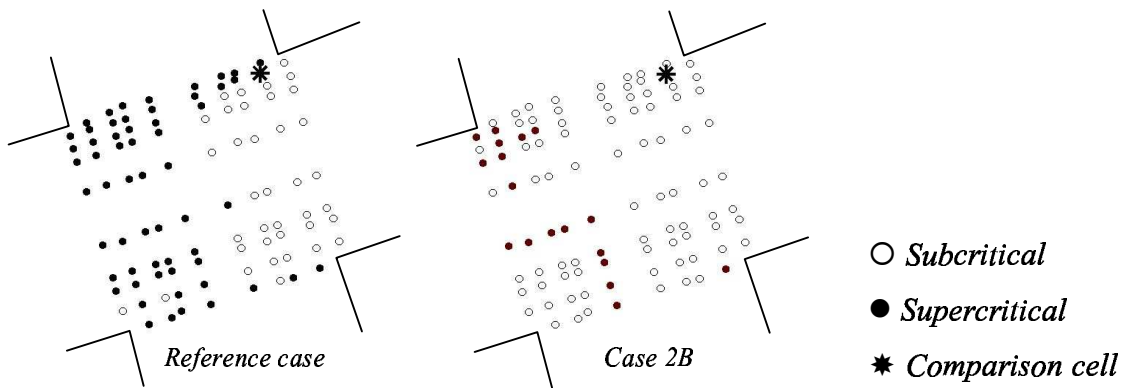
2



3

4 *Figure 8 : Linnigrams at point P1(Figure 1) for various parameter set cases.*

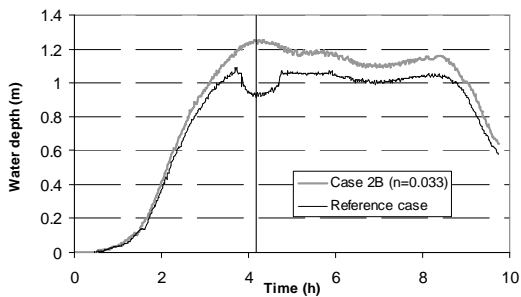
5



6 *Figure 9 : Flow regime patterns at the flood peak (t=4.1 hours) in one crossroad for Reference case and Case*

7 *2B*

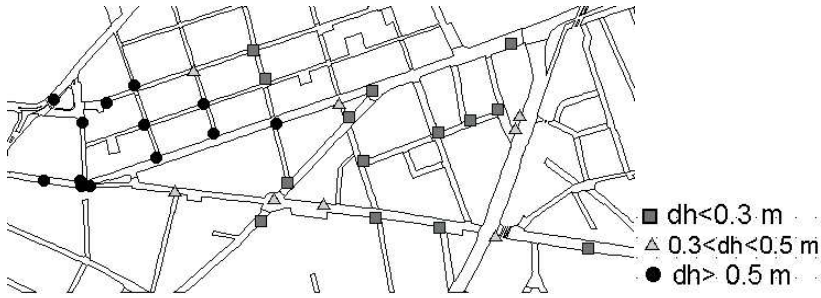
8



9

1 *Figure 10 : Limnigrams computed at the comparison cell of Figure 9 for Reference case and Case 2B.*

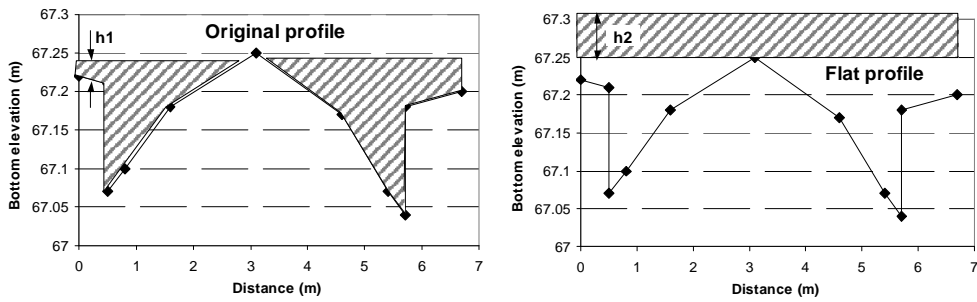
2



3

4 *Figure 11 : Comparison between the reference case and Case 3B computed water depths in the Central and Southern zones of the domain with $dh = h_{3B} - h_{reference}$.*

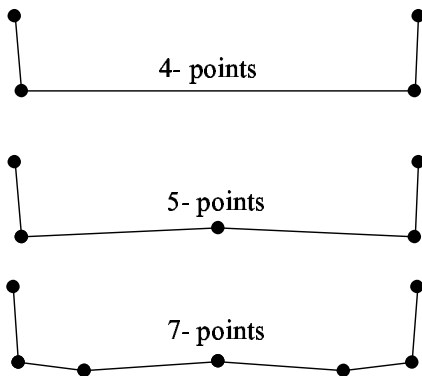
5



6

7 *Figure 12 : Increase in water depth using a flat profile description*

8

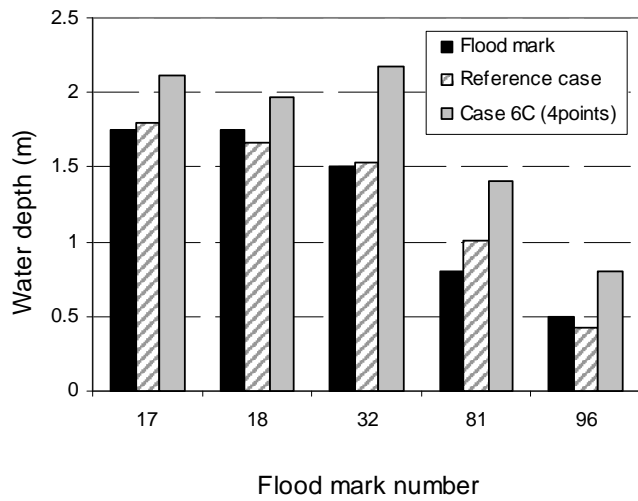


9

10 *Figure 13 : 7- 5- and 4-points simplified profiles*

11

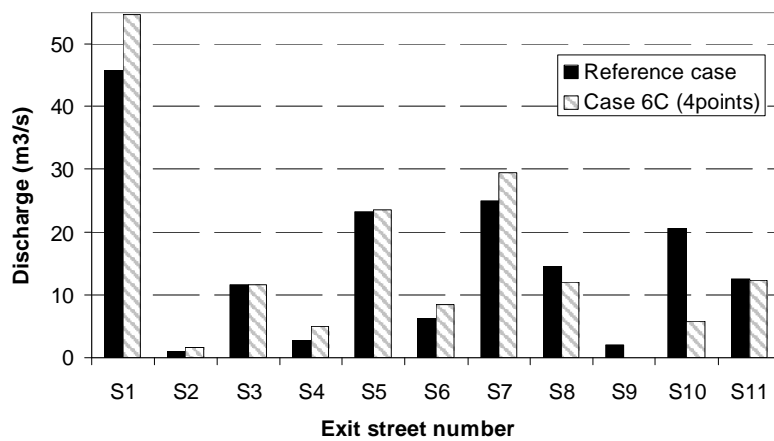
12



1

2 *Figure 14 : Comparison between flood mark and computed peak water depth for reference and 4-points cross-*
 3 *section calculation at supercritical small scale zones of the crossroads*

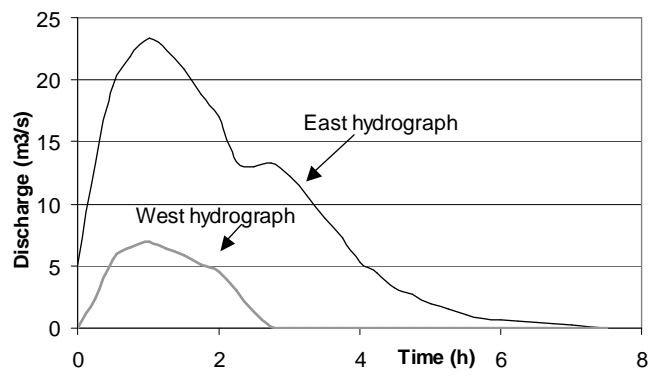
4



5

6 *Figure 15 : Comparison of flow rate distribution in the downstream end streets for reference and 4-points cases.*

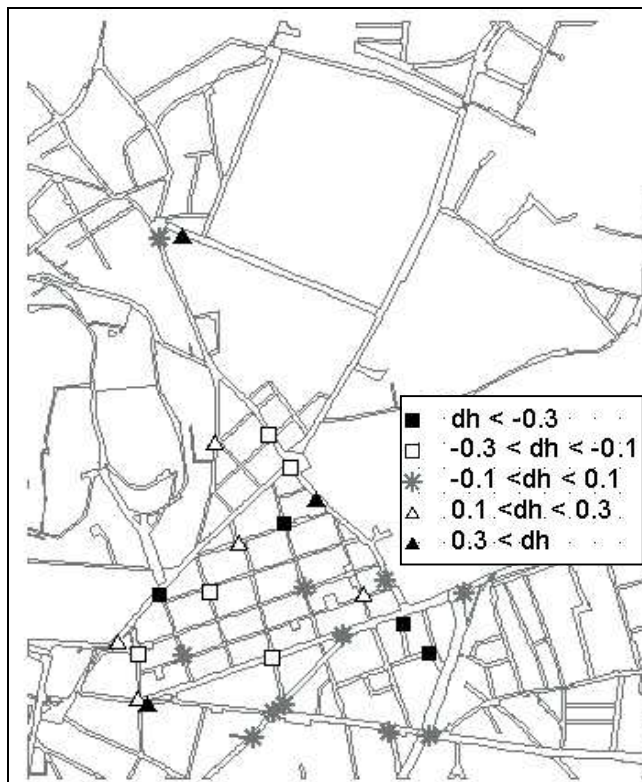
7



1

2 *Figure 16 : Flood hydrograph for September 2002 flood event after subtracting the sewer capacities.*

3



15 *Figure 17 : Comparison between peak water depths and measured flood marks*

16

1 **Tables**

2

		Northern zone	Central zone	Southern zone	Whole domain
Reference case	\overline{dh} (m)	0.04	-0.43	0.13	-0.13
	σ_{dh} (m)	0.56	0.54	0.43	0.53
Case 2B n=0.033	\overline{dh} (m)	0.17	-0.35	0.17	-0.04
	σ_{dh} (m)	0.57	0.54	0.44	0.53
Case 2C n=0.025 & n=0.05	\overline{dh} (m)	0.06	-0.23	0.14	-0.04
	σ_{dh} (m)	0.54	0.46	0.39	0.48
Case 3B S1, S2, S10 off	\overline{dh} (m)	0.05	-0.19	0.49	0.05
	σ_{dh} (m)	0.54	0.68	0.58	0.61
Case 6B 5-points/ section	\overline{dh} (m)	0.01	-0.36	0.29	-0.08
	σ_{dh} (m)	0.54	0.51	0.54	0.53
Case 6C 4-points / section	\overline{dh} (m)	0.07	-0.45	0.22	-0.11
	σ_{dh} (m)	0.64	0.7	0.56	0.65

3 *Table 1 : Comparison between computed and measured peak water depth for the reference case and some*

4 *important parameters modification. \overline{dh} is the average difference between computed and measured peak water*

5 *depths: $\overline{dh} = \frac{\sum dh}{n} = \frac{\sum (H_{computed} - H_{measured})}{n}$ with $H_{measured}$ the flood mark measurement, $H_{computed}$ the*

6 *computed peak water depth in the nearest cell and n is the number of flood marks (99 in this case). σ_{dh} is the*

7 *standard deviation of dh : $\sigma_{dh} = \sqrt{\frac{\sum (dh - \overline{dh})^2}{n}}$*

8

9

10

1

Parameter modification	(1)	(2)	(3)	Other impacts and remarks :
Increase input hydrographs <i>Case 1A</i>	X (↑)			Average increase of 12.5 cm if the flow rates are increased by 20%
Increase friction coefficient <i>Case 2B</i>	X (↑)	X	X	
Friction coefficient defined by zone <i>Case 2C</i>				The calibrated coefficient value improves the results in every zone
Change of downstream boundary condition numerical treatment <i>Case 3A</i>				Modification of discharge distribution in the downstream streets
Backwater effects from downstream zones : Blocking some exit streets. <i>Case 3B</i>				Global flow modifications in the whole Southern area
Flat street profile <i>Case 4A</i>	X (↑)		X	Similar increase of water depth in the three zones compared to Reference case
Simplified main crossroad <i>Case 4B</i>		X		Backwater effects upstream from the crossroad & flow pattern modifications
Local obstacle <i>Case 4C</i>				Strong local effects and slight downstream consequences
Simplified longitudinal mesh <i>Case 5A</i>		X	X	Modification of backwater effects in downstream filling zones
Simplified street profile (4 & 5-points cross-sections) <i>Cases 6B and 6C</i>	X (↑)	X	X	Simplification of the flow patterns in the street junctions
Considering the rain <i>Case 1B</i>	X (↑)			Limited impact due to small rain volumes compared to input hydrographs
Considering the storage areas <i>Case 1C</i>	X (↓)			Limited impact due to small volumes stored compared to input hydrographs
Diffusion coefficient <i>Case 2A</i>			X	Limited impact
Neglecting gutters (7-points cross-sections) <i>Case 6A</i>	X (↑)			Limited impact

2 *Table 2 : Impact of the main parameters in the sensitivity analysis with :*

3 *(1) = Global change of peak water depths (with ↑ = increase and ↓ = decrease of peak water depth)*

4 *(2) = Change in flow distribution at Faïta/Sully crossroad and to the downstream limit areas*

5 *(3) = Local flow regime change*